



## Molecular Crystals and Liquid Crystals Science and Technology. Section A. Molecular Crystals and Liquid Crystals

Publication details, including instructions for authors and subscription information:

<http://www.tandfonline.com/loi/gmcl19>

### Effect of Absolute Configuration on the Formation of TGB<sub>A</sub>\* Phase in Liquid Crystallines Containing Two Stereogenic Centres

Wen-Jiunn Hsieh<sup>a</sup> & Shune-Long Wu<sup>a</sup>

<sup>a</sup> Department of Chemical Engineering, Tatung Institute of Technology, Taipei, 10451, Taiwan R.O.C.

Version of record first published: 04 Oct 2006

To cite this article: Wen-Jiunn Hsieh & Shune-Long Wu (1997): Effect of Absolute Configuration on the Formation of TGB<sub>A</sub>\* Phase in Liquid Crystallines Containing Two Stereogenic Centres, Molecular Crystals and Liquid Crystals Science and Technology. Section A. Molecular Crystals and Liquid Crystals, 302:1, 253-269

To link to this article: <http://dx.doi.org/10.1080/10587259708041836>

PLEASE SCROLL DOWN FOR ARTICLE

Full terms and conditions of use: <http://www.tandfonline.com/page/terms-and-conditions>

This article may be used for research, teaching, and private study purposes. Any substantial or systematic reproduction, redistribution, reselling, loan, sub-licensing, systematic supply, or distribution in any form to anyone is expressly forbidden.

The publisher does not give any warranty express or implied or make any representation that the contents will be complete or accurate or up to date. The accuracy of any instructions, formulae, and drug doses should be independently verified with primary sources. The publisher shall not be liable for any loss, actions, claims, proceedings, demand, or costs or damages whatsoever or howsoever caused arising directly or indirectly in connection with or arising out of the use of this material.

## Effect of Absolute Configuration on the Formation of $TGB_A^*$ Phase in Liquid Crystallines Containing Two Stereogenic Centres

Wen-Jiunn Hsieh and Shune-Long Wu\*

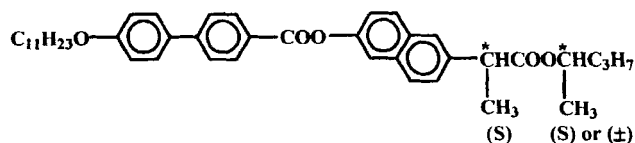
Department of Chemical Engineering, Tatung Institute of Technology, Taipei 10451, Taiwan R.O.C.

**Abstract** Our previous work has shown that a homologous series of chiral materials containing two stereogenic centres, (R)-2-pentyl (S)-2-(6-(4-(4-alkoxyphenyl)benzoyloxy-2-naphthyl)propionates (R,S)PmPBNP ( $m=7-14$ ), exhibited  $TGB_A^*$  phase. To understand the effect of relative configuration of two stereogenic centres at chiral tail on the appearance of  $TGB_A^*$  phase, two stereoisomers of (R,S)P11PBNP, (S,S)P11PBNP and ( $\pm$ ,S)P11PBNP were synthesized and their mesophases investigated. The results showed that both isomers also possessed  $TGB_A^*$  phase with the phase sequence of  $I-N^*-TGB_A^*-S_A^*-S_C^*-C$ . The temperature range of  $TGB_A^*$  phase in (R,S)-isomer was significantly larger than that in (S,S)-isomer, indicating the stability of  $TGB_A^*$  phase was affected by the relative spatial configuration of the second chiral centre at chiral tail. In addition, the temperature range of  $TGB_A^*$  phase in ( $\pm$ ,S)-isomer was larger than (S,S)-isomer, suggesting that an introducing methyl branched group at the external side of mono chiral centre could cause a weakening of smectic layer order and result in an occurrence of  $TGB_A^*$  phase. The measured  $P_s$  values in the  $S_C^*$  phase from the isomers, also indicated the absolute configuration of second chiral centre plays an important role in determining the magnitude of spontaneous polarization.

## INTRODUCTION

The optically active mesophases such as the blue phase<sup>1</sup>, ferroelectric<sup>2</sup>, ferrielectric<sup>3</sup> and antiferroelectric<sup>4</sup>  $S_C^*$  phases, and twisted grain boundary (TGB;  $TGB_A^*$ ,  $TGB_C$  and  $TGB_C^*$ ) phases<sup>5-8</sup> have been found in the liquid crystals system after the discovery of the first optically active  $N^*$  phase in 1888.<sup>9</sup> The investigation in the relationship between the chirality and liquid crystals, especially the TGB phases, has become one of most important research areas in this field. For examples, the systemic

investigations of propionates<sup>5-8, 11-12</sup> were obtained certain structural relationships on the formation the TGB phases and reviewed.<sup>10</sup> These factors divided according to the molecular structure of mesogen were the length of nonchiral terminal alkyl chain<sup>5,6</sup>, the length of external side terminal alkyl chain at chiral centre<sup>10</sup>, the effect of lateral substituted group on the core<sup>11</sup> and the linking groups<sup>10,12</sup> etc. However, only a few investigations<sup>13</sup> had been put forward to the effect of numbers of chiral centers and their absolute configurations on the occurrence of these mesophases. It should be noted that it is well known in the ferroelectric  $S_C^*$  phase. Our previous study<sup>14</sup> in a series homologous of materials, (R)-2-pentyl (S)-2-(6-(4-(4-alkoxyphenyl)benzoyloxy)-2-naphthyl)propionates, (R,S)PmPBNP ( $m=7-14$ ), containing two stereogenic centres showed an existence of  $TGB_A^*$  phase with the phase sequence:  $I-N^*-TGB_A^*-S_A^*-S_C^*$  for  $m=7-9$  and  $I-N^*-TGB_A^*-S_C^*$  for  $m=10-14$ . In order to understand the effect of the relative spatial configuration of the chiral tail on the formation of  $TGB_A^*$  phase, two stereoisomeric compounds of (R,S)P11PBNP, (S)-2-pentyl (S)-2-(6-(4-(4-undecyloxyphenyl)benzoyloxy)-2-naphthyl)propionates, (S,S)P11PBNP, and 2-pentyl (S)-2-(6-(4-(4-undecyloxyphenyl)benzoyloxy)-2-naphthyl)propionates, ( $\pm$ ,S)P11PBNP, were synthesized for the study. The relationship between the absolute configurations



on the appearance of  $TGB_A^*$  phase was established in terms of the mesomorphic properties of diastereomeric mixtures of (R,S)- and (S,S)- isomers. In addition, the

physical properties of ferroelectric S<sub>C</sub>\* were also measured and discussed.

### CHARACTERIZATION AND PREPARATION OF MATERIALS

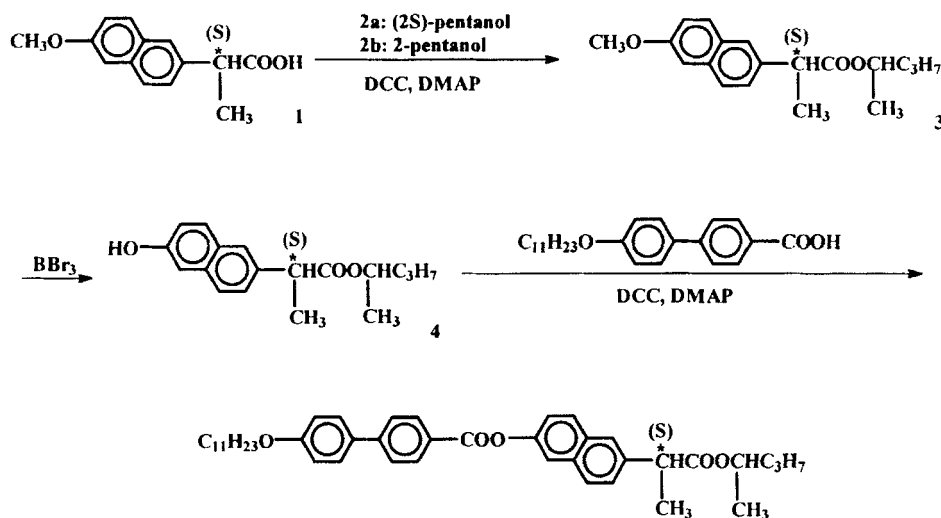
The chemical structures for intermediates and target compounds were analyzed by nuclear magnetic resonance spectroscopy using a JEOL EX-400 FT-NMR spectrometer. The purity was checked by thin-layer chromatography and further confirmed the purity of final products were done by the elemental analysis using a PERKIN-ELMER 2400 spectrometer. The magnitudes of the specific rotation were measured in dichloromethane using a JASCO DIP-360 digital polarimeter.

Mesophases of diastereomers and mixtures were principally identified by observing the textures in the glass slides, the homeotropic alignment cell with 7.5μm thickness purchased from Linkam Instr. Ltd and homogeneously alignment cell with 2μm thickness produced by the E.H.C. Co. using a NIKON MICROPHOT-FXA optical microscopy under crossed polarizers with a METTLER FP82-HT hot stage in connection with a METTLER FP80-HT heat controller. The ferroelectric phase was further identified by switching behaviour and dielectric property measurements<sup>15</sup> in parallel alignment liquid crystal cells with 2μm and 25μm thickness purchased from E.H.C. Co.

### Synthesis

The synthetic procedures for preparing chiral materials (S,S)P11PBNP and (±,S)P11PBNP were the same as that previously described for (R,S)P11PBNP<sup>14</sup> and were outlined in Scheme 1. The acid **1** was esterified with alcohol **2** in the presence of N,N'-dicyclohexyl carbodiimide (DCC) and 4-dimethylaminopyridine (DMAP) to produce an intermediate ester **3**. The methoxy group of this ester was

demethylated by the treatment of tribromoborane ( $\text{BBr}_3$ ), and the resulting hydroxy group of chiral compound **4** was subsequently esterified with 4-(4-undecyloxyphenyl)benzoic acid by the treatment of DCC and DMAP to produce the target compounds.



Scheme 1 Synthetic procedures for chiral materials (S,S)P11PBNP and ( $\pm$ ,S)P11PBNP  
(S)-2-Pentyl (S)-2-(6-methoxy-2-naphthyl)propionate 3a, (S,S)PMNP

(S)-2-Pentanol **2a** (27.5mmol), DCC (27.5mmol) and DMAP (2.5mmol) were added to a solution of acid **1** (25mmol) in 100ml dry dichloromethane. The reaction mixture was stirred continuously at room temperature for 3 days. The precipitates were filtrated and wash with dichloromethane. The filtrate was successively washed with 5% acetic acid, 5% aqueous sodium hydroxide and water and then dried by anhydrous magnesium sulfate. The product **3a**, (S,S)PMNP, was isolated by column chromatography over silica gel (70-230 mesh) with dichloromethane as eluent and dried in vacuo with the yield of 82% and used directly for the follow-up synthesis without purification.  $^1\text{H}$ -

NMR (400MHz, CDCl<sub>3</sub>):  $\delta$  0.7-1.7 (m, 13H, RCH<sub>2</sub>CH<sub>3</sub>), 3.87 (s, 3H, OCH<sub>3</sub>), 3.9-4.2 (q, 1H, ArCHCOO), 4.9-5.1 (m, 1H, COOCH), 7.1-7.8 (m, 6H, ArH).

2-Pentyl (S)-2-(6-methoxy-2-naphthyl)propionate 3b, ( $\pm$ ,S)PMNP

The synthetic procedures were the same as that for 3a. Yield: 90%. <sup>1</sup>H-NMR (400MHz, CDCl<sub>3</sub>):  $\delta$  0.7-1.7 (m, 13H, RCH<sub>2</sub>CH<sub>3</sub>), 3.9 (s, 3H, OCH<sub>3</sub>), 3.8-4.0 (q, 1H, ArCHCOO), 4.9-5.0 (m, 1H, COOCH), 7.0-7.8 (m, 6H, ArH).

(S)-2-Pentyl (S)-2-(6-hydroxy-2-naphthyl)propionate 4, (S,S)PHNP

Tribromoborane (2.5ml) was added to a solution of 3a (0.015mol) in 57ml dry dichloromethane at -20°C and further stirred for 5min. The reaction was then stirred 50min at 0°C. After diluting with dichloromethane (114ml), the solution was poured into a mixture of saturated ammonium chloride (57ml) and ice (57g). The organic layer was separated from aqueous layer and washed twice with brine-ice. The crude product 4a (S,S)PHNP was dried over anhydrous sodium sulfate and concentrated in vacuo. The product was purified twice by column chromatography over silica gel (70-230 mesh) with dichloromethane as eluent and then collected after recrystallization from hexane and dried in vacuo with the yield of 64%. <sup>1</sup>H-NMR (400MHz, CDCl<sub>3</sub>):  $\delta$  0.7-1.7 (m, 13H, RCH<sub>2</sub>CH<sub>3</sub>), 3.8 (q, 1H, ArCHCOO), 4.9-5.0 (m, 1H, COOCH), 5.26 (s, 1H, OH), 7.0-7.7 (m, 6H, ArH). Elemental analysis: Calc.: C, 75.50%; H, 7.74%. Found: C, 75.41%; H, 7.70%.

2-Pentyl (S)-2-(6-hydroxy-2-naphthyl)propionate 4b, ( $\pm$ ,S)PHNP

The synthetic procedures were the same as that for 4a. Yield: 70%. <sup>1</sup>H-NMR (400MHz, CDCl<sub>3</sub>):  $\delta$  0.7-1.7 (m, 13H, RCH<sub>2</sub>CH<sub>3</sub>), 3.8 (q, 1H, ArCHCOO), 4.9-5.0 (m, 1H, COOCH), 6.3 (s, 1H, OH), 7.0-7.7 (m, 6H, ArH). Elemental analysis: Calc.: C, 75.50%; H, 7.74%. Found: C, 75.62%; H, 7.72%.

(S)-2-Pentyl (S)-2-(6-(4-(4-undecyloxyphenyl)benzoyloxy)-2-naphthyl)propionate, (S,S)P11PBNP

compound **4a** (S,S)PHNP (1.05mmol) was reacted with 4-(4'-undecyloxyphenyl)benzoic acid (1.16mmol) by the treatment of DCC (1.26mmol) and DMAP (0.1mmol) in dry tetrahydrofuran (4ml) at room temperature for 5 days. After the work-up procedures, the product (S,S)P11PBNP was purified twice by column chromatography with dichloromethane as eluent and then collected after recrystallization from ethanol and dried in vacuo with the yield of 84%. <sup>1</sup>H-NMR (400MHz, CDCl<sub>3</sub>): δ 0.8-1.9 (m, 40H, RCH<sub>2</sub>CH<sub>3</sub>), 3.8 (q, 1H, ArCHCOO), 4.0 (t, 2H, OCH<sub>2</sub>), 4.9 (m, 1H, COOCH), 6.9-8.2 (m, 6H, ArH). Elemental analysis: Calc.: C, 79.61%; H, 8.61%. Found: C, 80.35%; H, 8.75%. Specific rotation [α]<sub>D</sub><sup>30</sup>(0.6g/100ml): +17.41°.

2-Pentyl (S)-2-(6-(4-(4-undecyloxyphenyl)benzoyloxy)-2-naphthyl)propionate, (±,S)P11PBNP

The synthetic procedures were the same as that for (S,S)P11PBNP. Yield: 90%. <sup>1</sup>H-NMR (400MHz, CDCl<sub>3</sub>): δ 0.1-1.8 (m, 40H, RCH<sub>2</sub>CH<sub>3</sub>), 3.8-3.9 (q, 1H, ArCHCOO), 4.1 (t, 2H, OCH<sub>2</sub>), 4.9-5.0 (m, 1H, COOCH), 7.1-8.2 (m, 6H, ArH). Elemental analysis: Calc.: C, 79.61%; H, 8.61%. Found: C, 79.58%; H, 8.68%. Specific rotation [α]<sub>D</sub><sup>30</sup>(0.6g/100ml): +5.63°.

Preparation of diastereomeric mixtures

Diastereomeric mixtures, except (±,S)-form, were prepared by mixing (R,S)-form and its diastereomeric compound (S,S)-form into a vial, adding 2-5ml dry dichloromethane into the vial and vigorously agitating the solution for about 2 min, and then dried in vacuo.

RESULTS

Mesomorphic properties

The samples sandwich-packed in two untreated glass slides were conducted in the heating and cooling runs at  $2^\circ\text{C}/\text{min}$  scanning rate for the microscopic observation. The mesophases and their corresponding phase transition temperatures principally identified by observing textures of the materials under crossed polarizing microscope were summarized in Table 1.

The mesophases of the  $(\pm, S)$ - and  $(S, S)$ - isomers were enantiotropic and possessed the same phase sequence:  $I-N^*-TGB_A^*-S_A^*-S_C^*-C$ . The  $TGB_A^*$  phase of  $(\pm, S)$ - and  $(S, S)$ - isomers was mediated between the  $N^*$  and the  $S_A^*$  transition unlike that of  $(R, S)$ -isomer was an intermediary phase between the  $N^*$  and the  $S_C^*$  transition. Examples of microscopic textures

Table 1 Phase transition temperatures ( $^\circ\text{C}$ ) of binary mixture of  $(S, S)$ - and  $(R, S)$ -isomers obtained by the microscopic observation on cooling

wt% of (S,S)- form	phase sequence						mp
	I	$N^*$	$TGB_A^*$	$S_A^*$	$S_C^*$	C	
0.00	• 137.1	• 134.2	•	-	116.3	• 55.8	• 86.0
2.86	• 136.8	• 134.0	• 129.3	• 116.8	•	65.4	• 85.7
5.62	• 136.9	• 133.9	• 129.2	• 115.0	•	60.6	• 85.2
10.57	• 136.6	• 133.8	• 128.2	• 115.4	•	62.8	• 84.9
31.03	• 136.9	• 133.4	• 129.3	• 113.5	•	62.8	• 83.2
50.00	• 135.3	• 131.5	• 128.6	• 110.7	•	65.3	• 81.1
71.29	• 134.8	• 130.9	• 128.5	• 107.9	•	64.4	• 80.2
85.12	• 132.5	• 129.6	• 127.3	• 107.3	•	65.1	• 83.1
100.00	• 129.4	• 127.2	• 126.1	• 106.8	•	73.6	• 87.1



observed from ( $\pm$ ,S)-isomer were displayed in Plates 1(a)-(d). The texture of  $N^*$  phase was characterized by the paramorphic and planar texture (Plate 1(a)). Cooling to the  $TGB_A^*$  phase, the paramorphic texture of  $N^*$  phase changed to the filament texture and the planar texture altered to more viscous and blurred planar texture (Plate 1(b)). When cooling to  $S_A^*$  phase, the focal-conic and homeotropic texture coexisted with filament texture (Plate 1(c)), appeared to be resembled to that observed by Bouchta et al.<sup>12</sup> Continuously lowering the temperature to the  $S_C^*$  phase, the disclination lines appeared in the focal-conic region and the filament texture disappeared and converted to the iridescent planar texture (Plate 1(d)). Similar mesomorphic textures were also observed in the (S,S)-isomer and the diastereomeric mixtures.

Mesophases of ( $\pm$ ,S)-isomer were also characterized by the textures (Plates 2(a)-(d)) in the cells with parallel alignment layer. The microscopic texture exhibited significantly colored Bragg-like reflection with shorter selective reflecting wavelength of light in the  $N^*$  phase and longer reflecting wavelength of light in the  $TGB_A^*$  phase as shown in Plates 2(a) and 2(b), respectively. When the temperature closed to the  $TGB_A^*-S_A^*$  transition, the selectively reflecting phenomena were no longer observed due to the variation of helical pitch in the  $TGB_A^*$  phase. Upon further cooling, a poorly aligned texture (Plate 2(c)) of  $S_A^*$  phase resembled to that observed by Nishiyama et al.<sup>16</sup> was found. This poor alignment of the  $S_A^*$  phase was attributed due to the twist ordering of the molecules in the  $TGB_A^*$  phase. The textures of  $S_C^*$  phase obtained from ( $\pm$ ,S)- and (S,S)- isomers (Plate 2(d)) were different with respect to the parquet texture (Plate 3(a)) obtained from (R,S)-isomer. The parquet texture could be gradually altered to the surface-stabilized state when the electric field was steadily and increasingly applied as shown in Plates 3(b) at 9.5V, 3(c) at 14.2V and 3(d) at -14.2V. The field-

induced texture was irreversible upon removal of electric field. The threshold hold voltages for the (R,S)-, ( $\pm$ ,S)- and (S,S)- isomers were 6.5V, 4.9V and 3.8V, respectively.

#### Miscibility study

Further investigation on the effect of absolute configuration of the second chiral centre on the occurrence of  $TGB_A^*$  phase was conducted by investigating the mesomorphic properties of diastereomeric mixtures. The mesophases and corresponding phase transition temperatures were also summarized in the Table 1. The phase diagram of the mixtures was plotted in Figure 1. It showed that the clearing points were

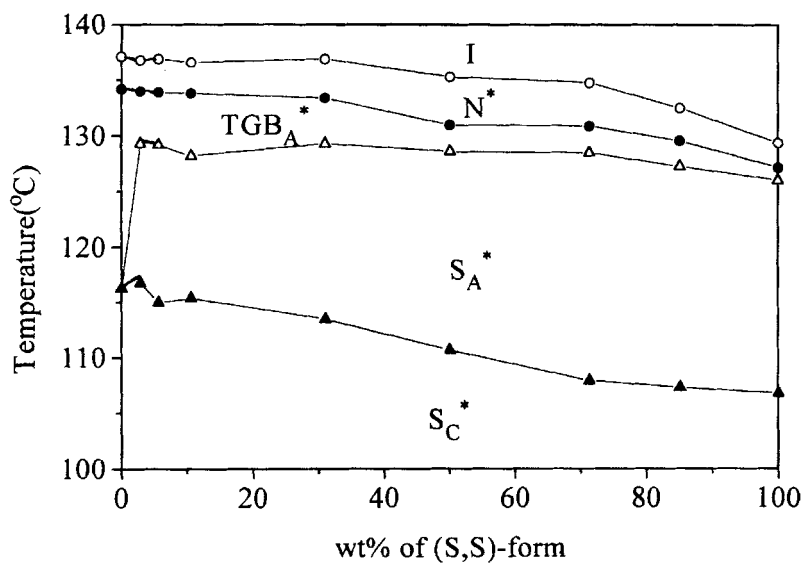


Figure 1 Phase diagram of binary mixtures of the (S,S)- and (R,S)- isomers.

decreased as the increasing concentration of (S,S)-isomer. Similar trends were also observed for all transition temperatures. The figure also indicated that the  $N^*$ ,  $TGB_A^*$  and  $S_C^*$  phases were continuously miscible in the phase diagram, suggesting that

the helix senses of these phases in (S,S)- and (R,S)-isomers were the same. Furthermore, it was worth to note that the most striking feature was the temperature range of  $TGB_A^*$  phase dramatically and sharply suppressed by adding a small quantity of (S,S)-isomer into the (R,S)-isomer.

#### Spontaneous Polarization of $S_C^*$ phase

The physical properties of the ferroelectric  $S_C^*$  phase such as direction and magnitude of spontaneous polarization ( $P_s$ ) for (R,S)-isomer and its diastereomers were measured as a function of temperature on cooling in the 2  $\mu$ m thickness homogeneously aligned cells. The directions of spontaneous polarization for all isomers were all negative (-) detected by the switching studies.<sup>17</sup> All stereoisomers showed the similar tendency in temperature dependence of spontaneous polarization. The magnitudes of spontaneous polarization as a function of reduced temperature from the Curie point ( $T_c$ ) shown in Figure 2, indicated an order of (S,S)- > ( $\pm$ ,S)- > (R,S)- isomers.

#### DISCUSSION

The experimental results indicated that the temperature range of  $TGB_A^*$  phase of (R,S)-, ( $\pm$ ,S)- and (S,S)- isomers were 17.9°, 2.9° and 2.1°C, respectively. Since the formation and stability of  $TGB_A^*$  phase have been reported to be chirality dependent<sup>18</sup>, the (R,S)-isomer should possess a larger degree of molecular chirality than its diastereomers (S,S)-isomer. Moreover, considering the pre-transitional effect caused by the underlying  $S_C^*$  phase<sup>19</sup>, the stability of  $TGB_A^*$  phase of (R,S)-isomer should be greater than that of (S,S)-isomer. This result was the same as those of the phenyl-

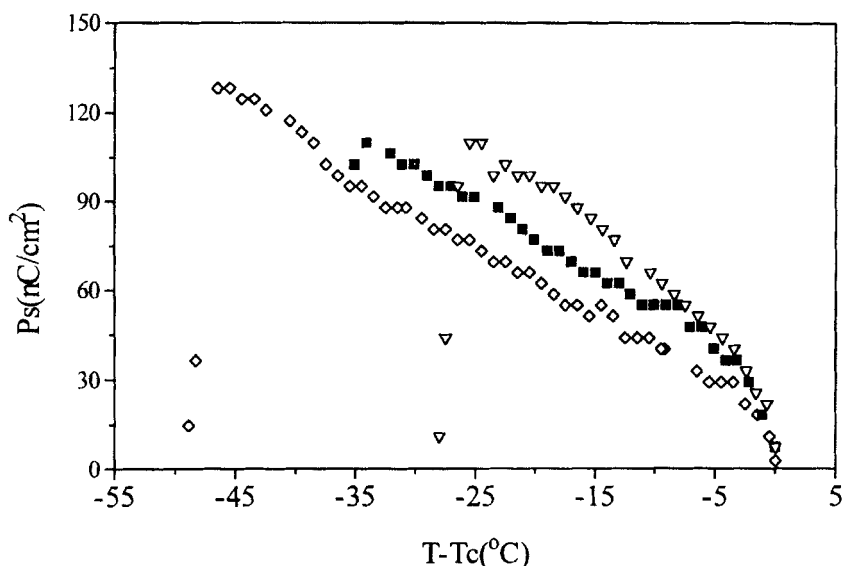


Figure 2 Temperature dependence of spontaneous polarization ( $P_s$ ) of (R,S)-;  $\circ$ , ( $\pm$ ,S)-;  $\blacksquare$  and (S,S)-;  $\triangle$ .

propionate esters derived from isoleucine.<sup>13</sup> However, as comparing the temperature range of  $TGB_A^*$  phase between ( $\pm$ ,S)-isomer and (S,S)- isomer, the chirality might not be the only cause for the occurrence of  $TGB_A^*$  phase. It was apparent that an introducing methyl branched group at the external side of the first chiral centre could increase the steric hindrance<sup>10</sup> to affect the molecular packing such that weaken the smectic layer order and form a  $TGB_A^*$  phase. Furthermore, a sharply decreasing the  $TGB_A^*$  temperature range as a small quantity of (S,S)-isomer was added to the (R,S)-isomer, demonstrated that the stability the  $TGB_A^*$  phase strongly depended on the relative spatial configuration and optical purity of the second chiral centre at the chiral tail.

The direction of  $P_s$  predicted by using the Boulder model<sup>20</sup>, as shown in

Figure 3, suggested that the direction should be negative (-), in agreement with the

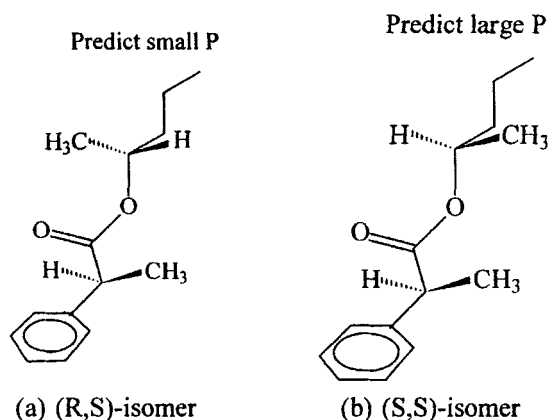


Figure 3 Boulder model for the predication of the relative spatial configuration on the diastereomeric compounds (a) (R,S)- and (b) (S,S)-isomers

measured results. Moreover, this figure also showed an obvious difference for diastereomers in relative spatial configuration at chiral tail, such that the effective transverse dipole moment produced by two methyl groups and dipolar carbonyl group<sup>21</sup> for the (R,S)-isomer was smaller than that for (S,S)- and ( $\pm$ ,S)- isomers in consistent with the measured magnitudes of  $P_s$  values. This was to suggest that the absolute configuration of second chiral centre might not affect, to some degree, the magnitude of transverse dipole moment.

## CONCLUSION

We have demonstrated that the formation and the stability of the  $TGB_A^*$  phase remarkably depended on the relative spatial configuration and optical purity of the chiral materials containing two stereogenic centres. Moreover, an introducing methyl

branched group to the external side of the first chiral centre at the chiral tail could cause a weakening of the smectic layer order and result in the formation of TGB<sub>A</sub>\* phase.

### ACKNOWLEDGEMENTS

The authors wish to appreciate the National Science Council (NSC84-2215-E-036-001) and ChungHwa Picture Tubes, LTD. for the financial support for this work.

### REFERENCES

1. H. Stegmeyer and K. Bergmann, in Liquid Crystals of One- and Two-Dimensional Order (Springer, Berlin, 1980), edited by W. Helfrich and A. Heppke, p. 161; H. Stegmeyer, T.H. Blumel, K. Hiltrop, H. Onusseit and F. Prosch, Liq. Cryst., **1**, 3 (1986); P.P. Crooker, Liq. Cryst., **5**, 751 (1989).
2. R.B. Meyer, L. Liebert, L. Strezlecki and P. Keller, J. Phys. Lett. (Paris), **36**, L69 (1975).
3. T. Isozaki, H. Takezoe, A. Fukuda, Y. Suzuki and I. Kawamura, J. Mater. Chem., **4**, 237 (1994).
4. A. Chandani, T. Hagiwara, Y. Suzuki, Y. Ouchi, H. Takezoe and A. Fukuda, Jpn. J. Appl. Phys., **27**, L729 (1989).
5. J.W. Goodby, M.A. Waugh, S.M. Stein., E. Chin, P. Pindak and J.S. Patel, Nature (London), **337**, 449 (1987).
6. J.W. Goodby, M.A. Waugh, S.M. Stein, E. Chin, P. Pindak and J.S. Patel, 1989, J. Am. Chem. Soc., **111**, 8119 (1989).
7. H.T. Nguyen, A. Bouchta, L. Navailles, P. Barois, N. Isaert, R.J. Twieg, A. Maaroufi and C. Destrade, J. Phys. II France, **2**, 1889 (1992).
8. M.A. Waugh., S.M. Stein, E. Chin and J.W. Goodby, Liq. Cryst., **11**, 135 (1992).
9. F. Reinitzer, Monatsh. Chem., **2**, 421 (1888); O.Z. Lehmann, Phys. Chem. (Leipzig), **4**, 462 (1989).
10. J.W. Goodby, A.J. Slaney, C.J. Booth, I. Nishiyama, J.D. Vuijk, P. Pstyrwg and K.J. Toyne, Mol. Cryst. Liq. Cryst., **243**, 231 (1994).
11. C.J. Booth, J.W. Goodby, K.J. Toyne, D.A. Dunmur and J.S. Kang, Mol. Cryst. Liq. Cryst., **260**, 39 (1995).; H.T. Nguyen, R.J. Twieg, M.F. Nabor and I. Isaert, Ferroelectrics, **121**, 187 (1991).
12. A. Bouchta, H.T. Nguyen, M.F. Achard, F. Hardouin, C. Destrade, R.J. Twieg, A. Maaroufi, and N. Isaert, Liq. Cryst., **12**, 575 (1992).; A. Bouchta, H.T. Nguyen, L. Navailles, P. Barois, C. Destrade, A. F. Bougrioua and N. Isaert., J. Mater. Chem., **5**, 2079 (1995).

13. A.J. Slaney, M. Watson and J.W. Goodby, J. Mater. Chem., **5**, 2145 (1995).
14. S.L. Wu and W.J. Hsieh, Liq. Cryst., Submitted for publication.
15. Y. Takanishi, H. Takezoe, A. Fukuda, H. Komura and J. Watanabe, J. Mater. Chem., **2**, 71 (1992).
16. I. Nishiyama and A. Yoshizawa, Liq. Cryst., **17**, 555 (1994).
17. J.W. Goodby et al., Ferroelectric Liquid Crystals: Principle, Properties and Applications ( Gordon and Breach, Philadelphia, 1991), p. 190.
18. A.J. Slaney and J.W. Goodby, Liq. Cryst., **9**, 849 (1991).
19. P.G. De Gennes, Solid State Commum., **10**, 753 (1972).
20. D.M. Walba, Adv. in the Synth. and React. of Solid, **1**, 173 (1991).
21. J.S. Patel and J.W. Goodby, Opt. Eng., **26**, 273 (1987); K. Yoshino, M. Ozaki, T. Sakurai, K. Sakamoto and M. Hanma, Jpn J. Appl. Phys. Lett., **20**, L175 (1984).

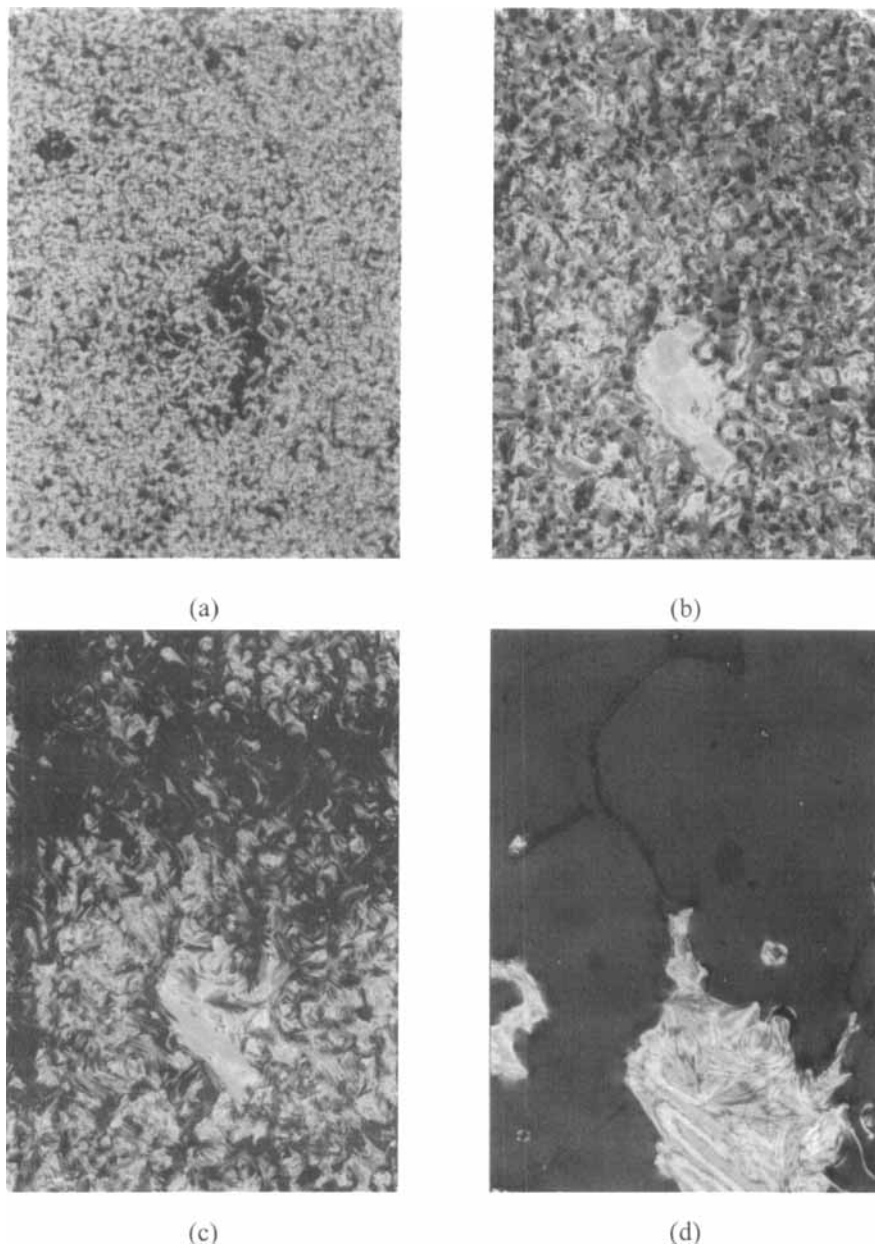


Plate 1 (a) The paramorphotic and Grandjean texture of  $N^*$  phase at 133.8°C (X100), (b) the Grandjean and filament texture of  $TGB_A^*$  phase at 129.7°C (X200), (c) the focal-conic and homeotropic texture of  $S_A^*$  phase at 127.9°C (X200) and (d) the broken focal-conic with striated lines and planar texture of  $S_C^*$  phase at 80.3°C (X400) of  $(\pm, S)$ -isomer in slides under crossed polarizers microscope. (See Color Plate IV).



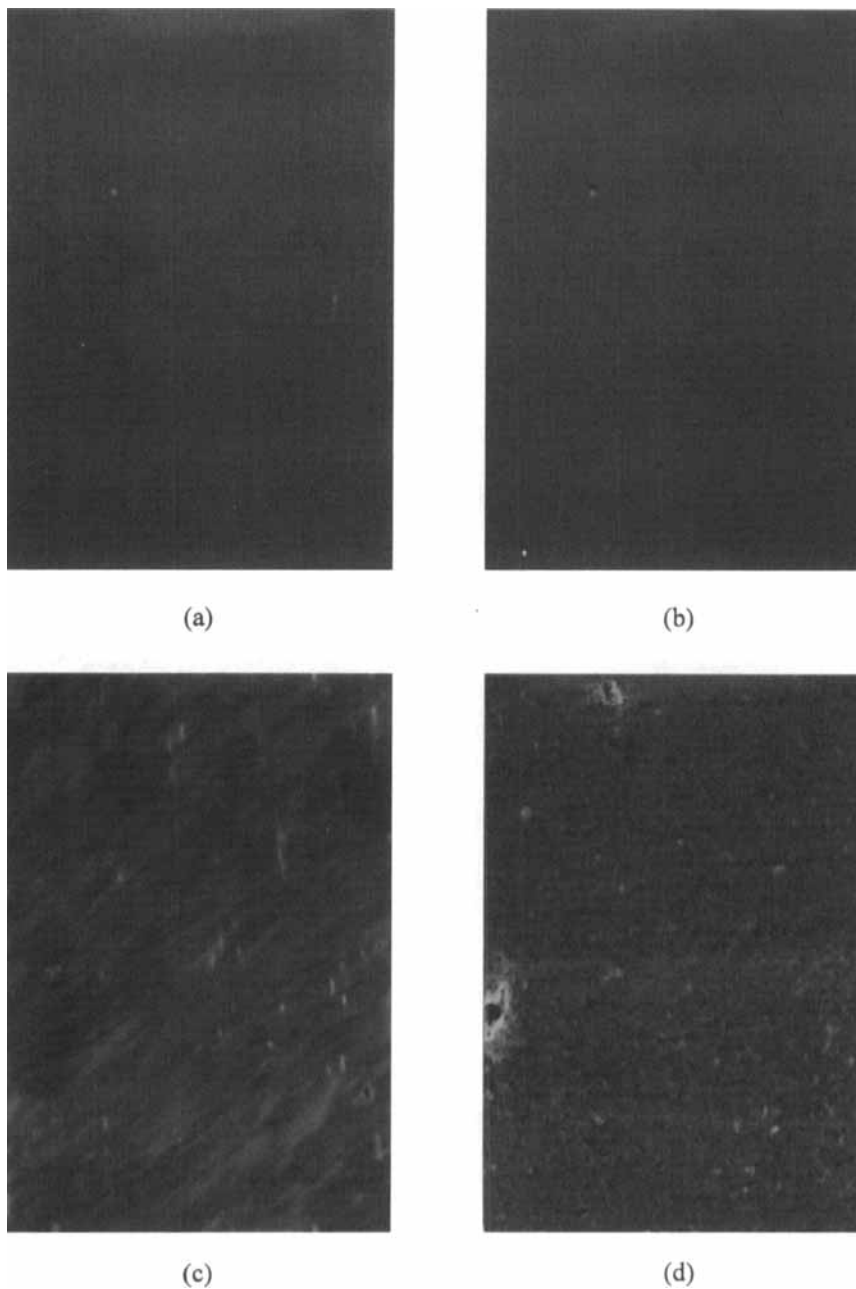


Plate 2 The mesophase texture of (±,S)-isomer observed in the cell with homogeneously aligned layer under crossed polarizers microscope. (a) N\* phase at 130.8°C (X100), (b) TGB<sub>A</sub>\* phase at 128.5°C (X100), (c) S<sub>A</sub>\* phase at 126.2°C (X100) and (d) S<sub>C</sub>\* phase at 94.3°C (X100). (See Color Plate V).

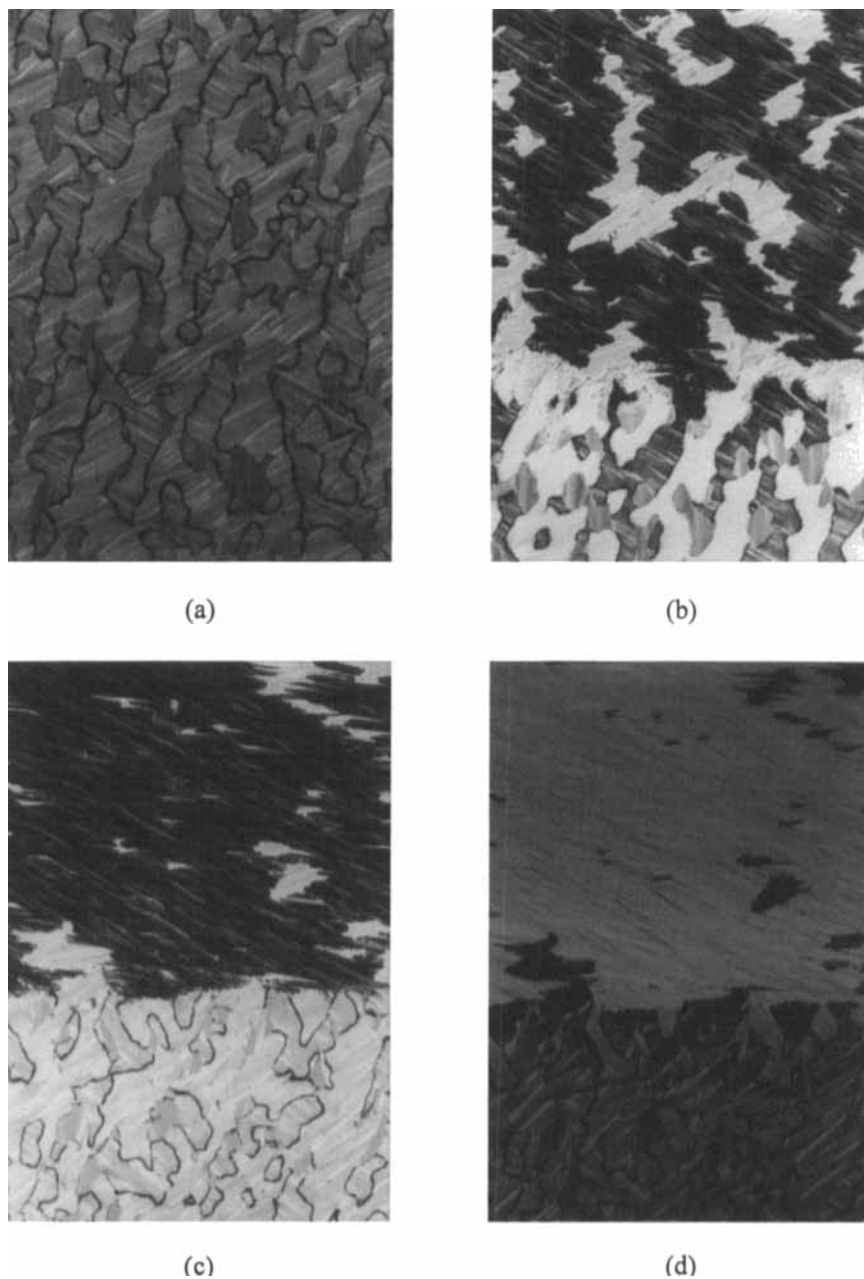


Plate 3 The texture of  $S_C^*$  phase of (R,S)-isomer with (upper part) and without (bottom part) electrode under applied voltage at  $T-T_c=-5^\circ\text{C}$ . (a) 0V, (b) 9.5V (c) 14.16V and (d) -14.16V. (See Color Plate VI).